Electronic Supplementary Material (ESI) for Journal of Materials Chemistry A

Surface-Engineered Mesoporous Pt Nanodendrites with Ni Dopant for Highly Enhanced Catalytic Performance in Hydrogen Evolution Reaction

Lu Li, [a] *Shan Wang,* [a] *Laifei Xiong,* [a] *Bin Wang,* [a] *Guang Yang* [a*] *and Shengchun Yang* [a, b*]

[†]School of Science, Key Laboratory of Shaanxi for Advanced Materials and Mesoscopic Physics, State Key Laboratory for Mechanical Behavior of Materials, Xi'an Jiaotong University, Xi'an, 710049, People's Republic of China

[‡]Collaborative Innovation Center of Suzhou Nano Science and Technology, Suzhou Academy of Xi'an Jiaotong University, 215000, Suzhou, People's Republic of China

Reagents

Platinum (II) acetylacetonate [Pt(acac)$_2$, AR.] and nickel(II) acetylacetonate [Ni(acac)$_2$, AR.] were obtained from the Kunming institute of precious metals. Polyvinylpyrrolidone (PVP, MW of ~8 000) was purchased from China national pharmaceutical group corporation. Ethanol (AR.) and 2-propanol (AR.) were purchased from Tianjin Fuyu Chemical Reagent. phemethylol was purchased from Tianjin Tianli Chemical Reagents. Deionized (DI) water (18.25 MΩ) used in experiment was prepared by passing through an ultra-pure purification system. All the materials were used as received without further purification.

Characterization

The morphology and structure of the as-prepared nanoparticles were characterized by transmission electron microscopy (TEM, JEOL JEM-2100) with an acceleration voltage of 200 kV, and high-resolution transmission electron microscopy (HRTEM, FEI Titan G2 60−300 equipped with image spherical aberration corrector) at 300 kV. The high angle annular dark field scanning transmission electron microscopy (HAADF-STEM) and energy-dispersive X-ray spectroscopy (EDS) analysis were performed on a JEOL ARM 200F. All TEM samples were prepared by a drop of the liquid onto lacy carbon-coated copper grids and natural drying. The phase and crystalline structures of the products were characterized by X-ray diffractometer (XRD, Bruker, AXS) using a Cu Ka radiation. The composition of 3D PtNi/Pt DNPs was determined by inductively coupled plasma emission spectroscopy (ICP-AES 5300)

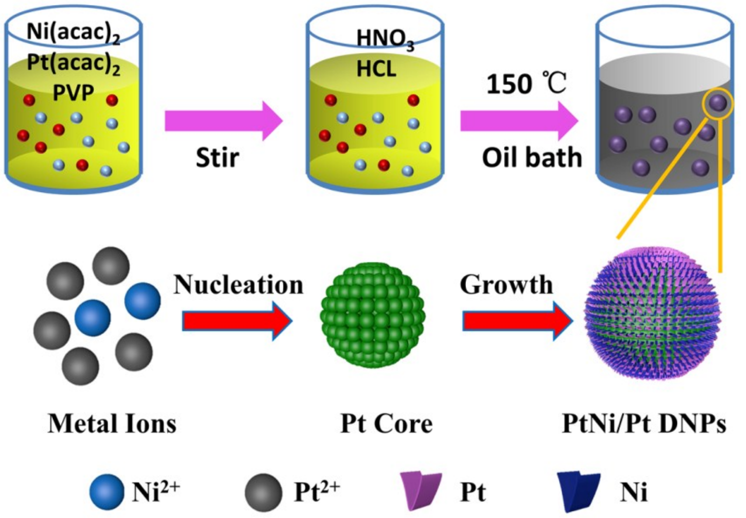

Fig. S1 Schematic illustration of the synthesis of PtNi/Pt DNPs

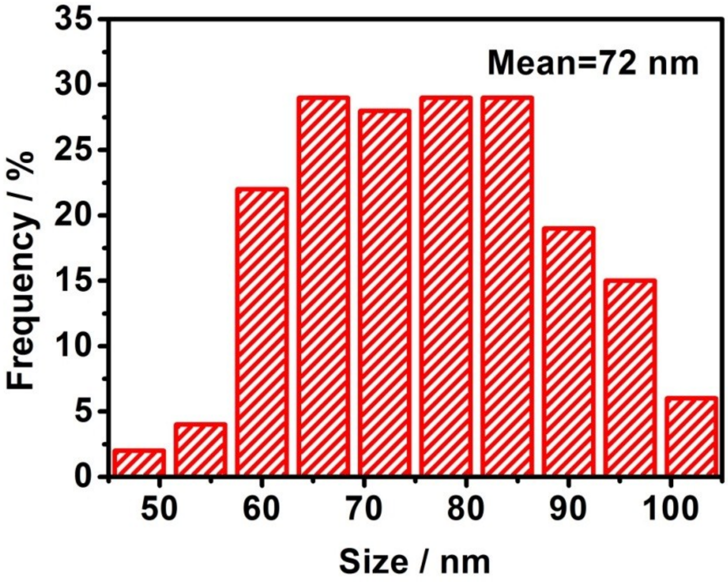

Fig. S2 Histogram of diameter distribution of PtNi/Pt DNPs

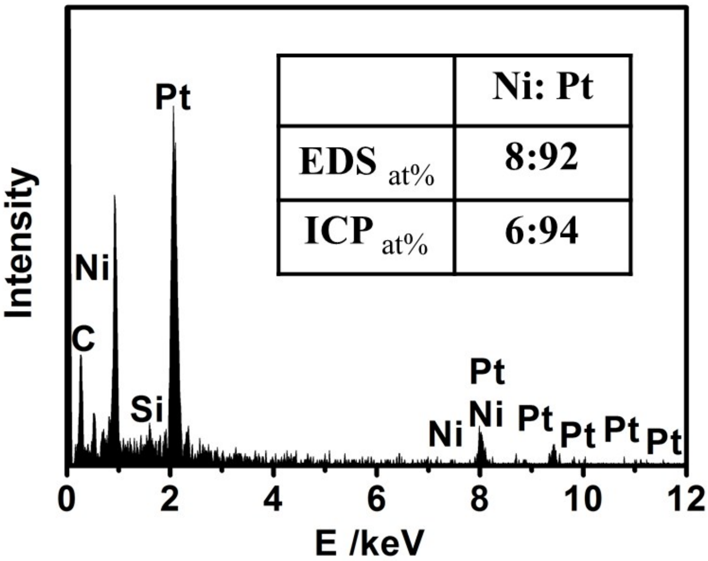

Fig. S3 EDS of PtNi/Pt DNPs (inset: atomic ratio of Ni and Pt measured by EDS and ICP, respectively)

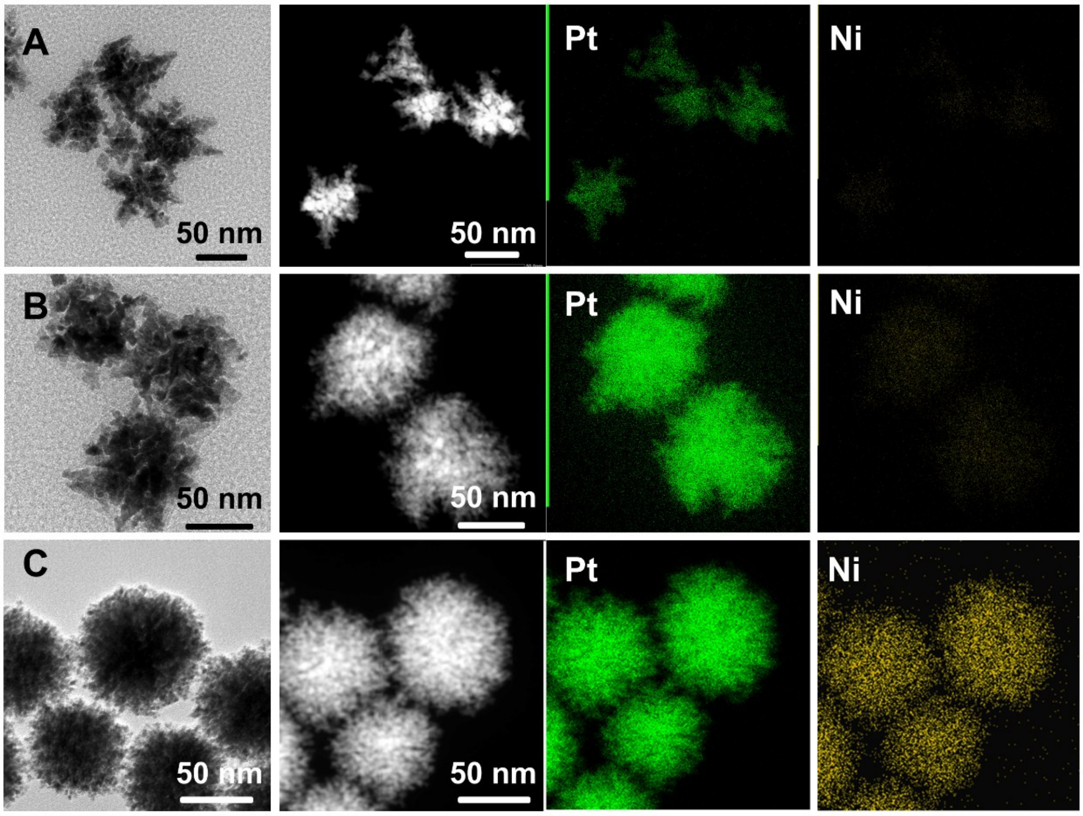

Fig. S4 TEM, HADDF-STEM images and EDX elemental maps of the reaction intermediates collected at (A) 1 h, (B) 3 h and (C) 6 h, respectively.

Table. S1 Calculation of lattice parameters in presence and absence of Ni.

substance	a/Å
Pure Pt	3.923
PtNi/Pt DNPs	3.895

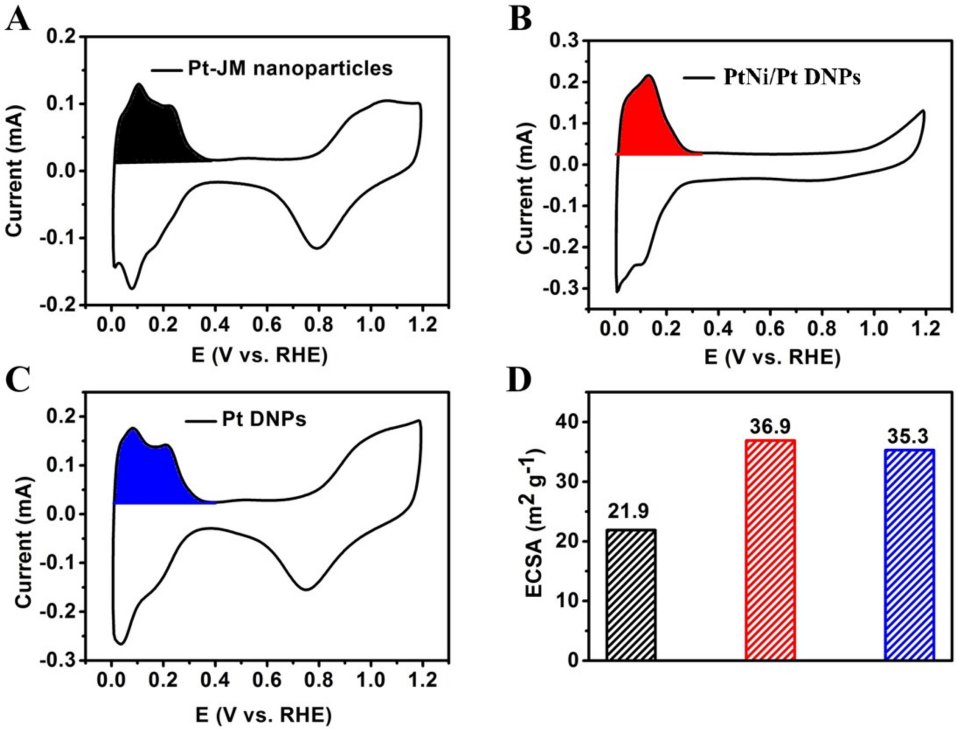

Fig. S5 Cyclic voltammetry curves of (A) Pt-JM NPs, (B) PtNi/Pt DNPs and (C) Pt DNPs in N_2-saturated 0.5 M H_2SO_4 with a scan rate of 50 mV s^{-1}, and (D) comparison of ECSA at Pt-JM NPs (black), PtNi/Pt DNPs (red), Pt DNPs (blue)

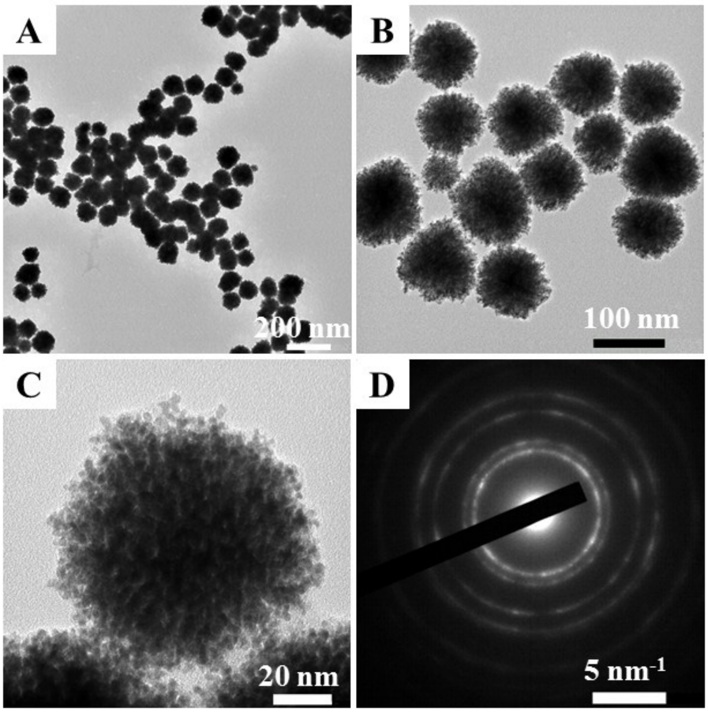

Fig. S6 Morphological and structural characterization of as-prepared Pt DNPs. (A) large-area TEM image, (B) TEM image, (C) TEM image of single nanoparticle, and (D) SAED pattern of Pt DNPs

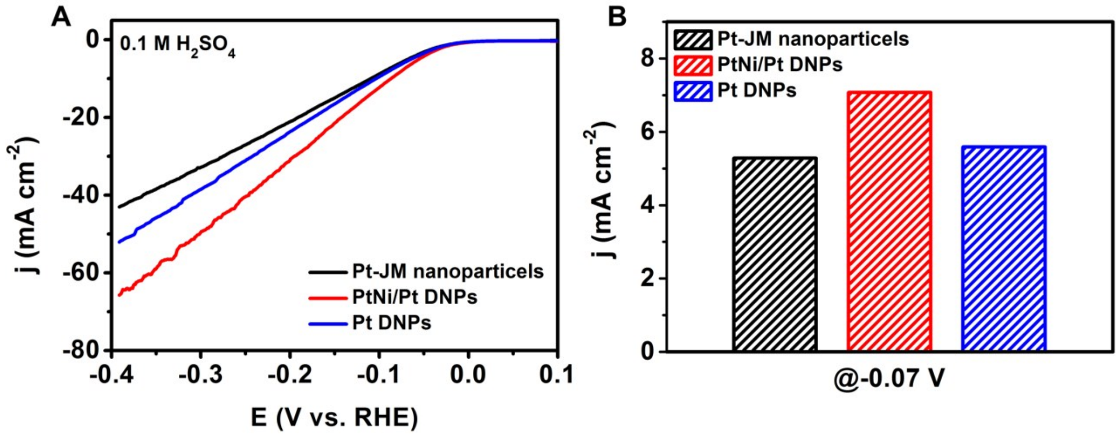

Fig. S7 (A) HER polarization curves of PtNi/Pt DNPs, Pt DNPs and commercial Pt-JM in 0.1 M H_2SO_4 (pH = 0.7). (B) Histograms of comparative current densities at -0.07 V versus RHE.

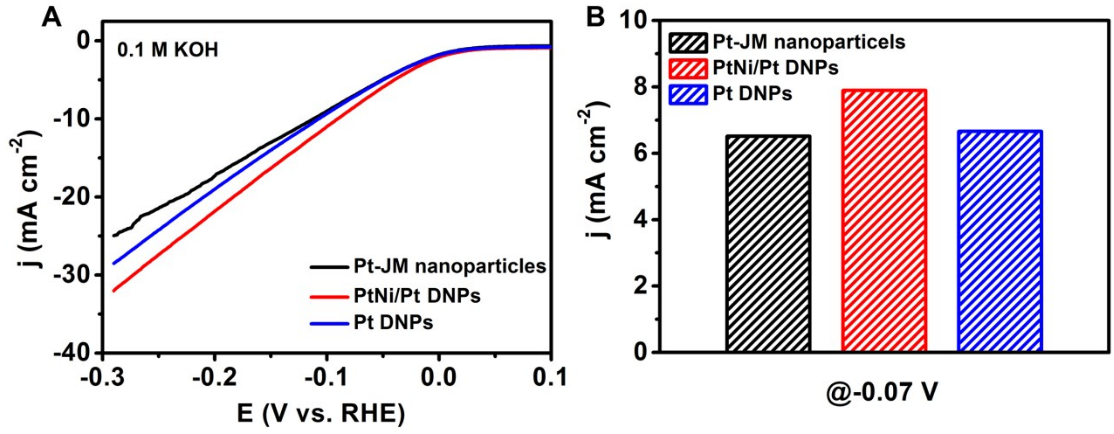

Fig. S8 (A) HER polarization curves of PtNi/Pt DNPs, Pt DNPs and commercial Pt-JM in 0.1 M KOH (pH = 13). (B) Histograms of comparative current densities at -0.07 V versus RHE.

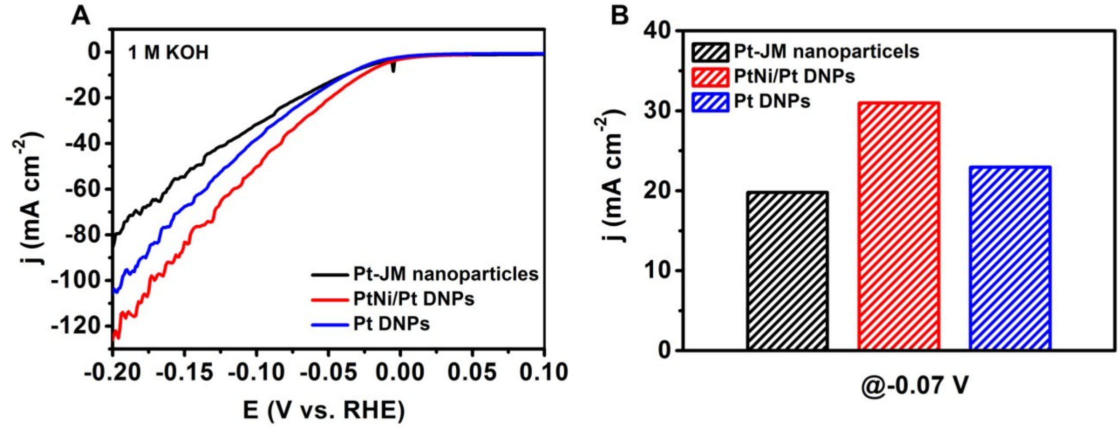

Fig. S9 (A) HER polarization curves of PtNi/Pt DNPs, Pt DNPs and commercial Pt-JM in 1 M KOH (pH=14). (B) Histograms of comparative current densities at -0.07 V versus RHE.

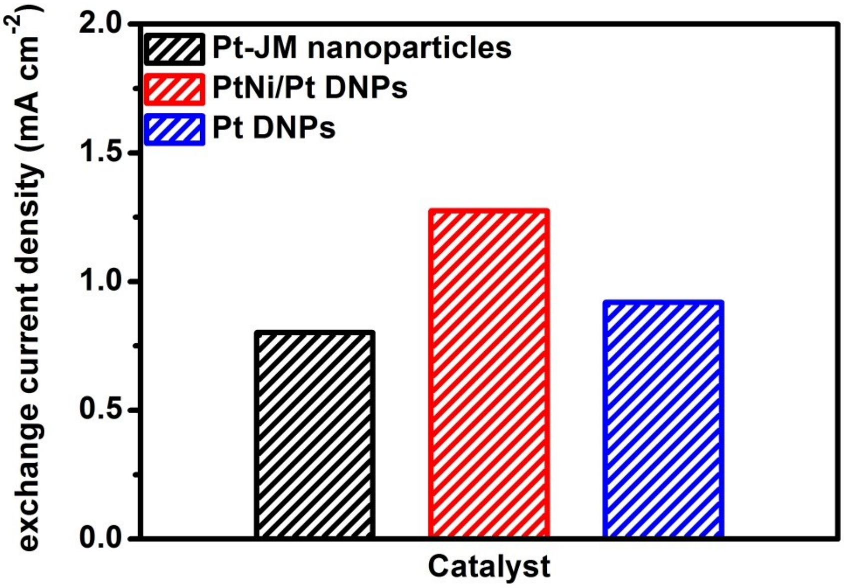

Fig. S10 Comparison of exchange current densities of commercial Pt-JM, PtNi/Pt DNPs and Pt DNPs.

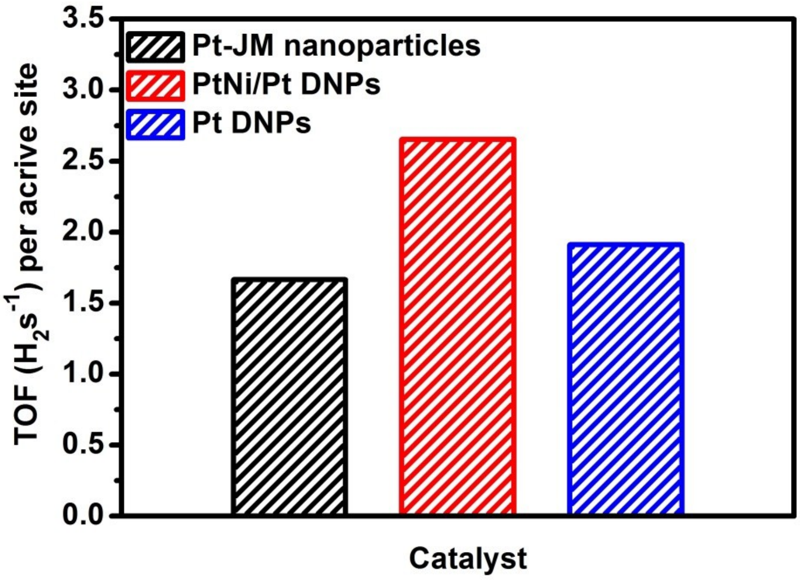

Fig. S11 Comparison of turnover frequency of commercial Pt-JM, PtNi/Pt DNPs and Pt DNPs.

Turnover frequency (TOF) is calculated from exchange current densities using the following equation:[1]

$$\text{TOF } (s^{-1}) = (j_0, \text{ A cm}^{-2}) / [(1.5\times10^{15} \text{ sites per cm}^2) \times (1.602\times10^{-19} \text{ C/e}^{-1}) \times (2 \text{ e}^{-1}/H_2)]$$

The site density of Pt is 1.5×10^{15} sites per cm^2.

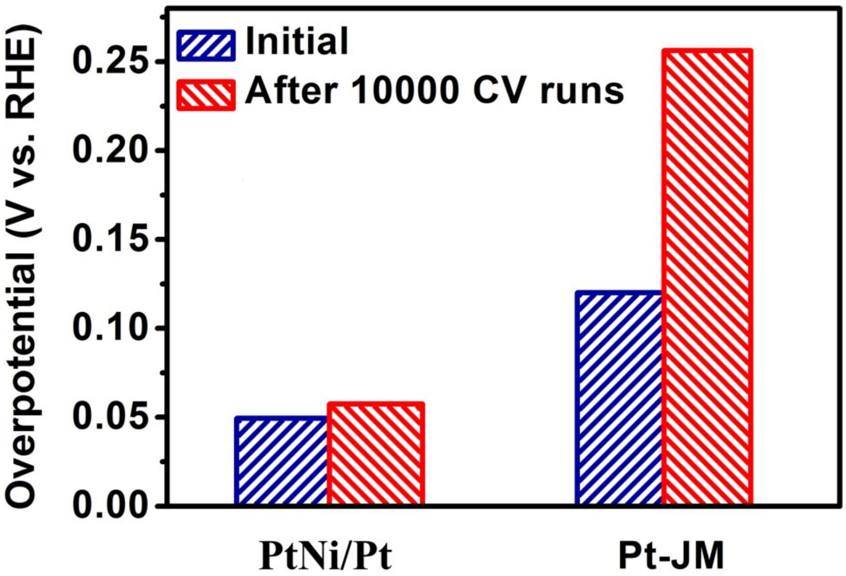

Fig. S12 Overpotential at *j*=100 mA cm^{-2} of the PtNi/Pt DNPs and commercial Pt-JM NPs for the HER before and after 10000 cycles

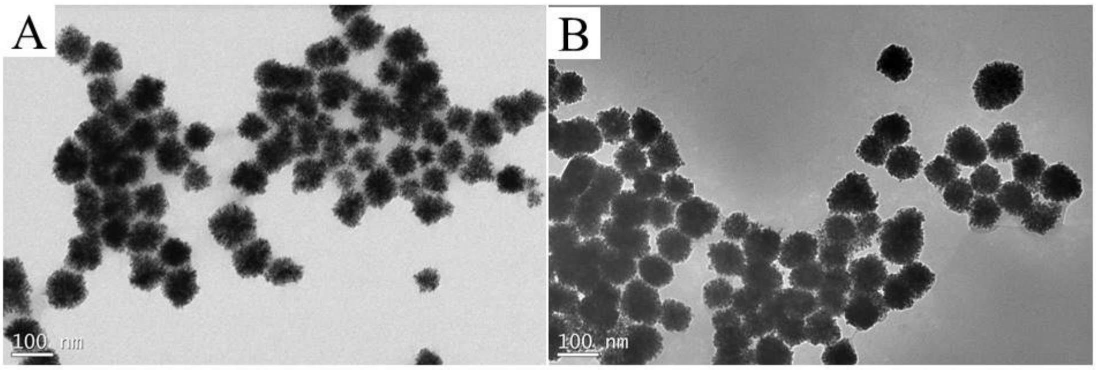

Fig. S13 TEM images of PtNi/Pt DNPs of (A) before and (B) after long-term durability test

Table S2. Summary of HER properties of the high performance electrode materials reported in recent literatures in 0.5 M H_2SO_4. (The current densities in the table are normalized to the geometric area of electrode). *The value is evaluated from the polarization curves exhibited in the literature.

Catalysts	Loading amount (μg cm^{-2})	Overpotential (mV) @				Tafel slope (mV dec^{-1})	Ref.
		10 mA cm^{-2}	20 mA cm^{-2}	50 mA cm^{-2}	100 mA cm^{-2}		
PtNi/Pt	51	21	29	38	46	23	This work
ALD 50 Pt/NGNs	76.5	40	50*	-----	-----	29	2
Pt@PCM	----	105	-----	-----	-----	65.3	3
PdCu@Pd NCs	140	68	90*	120*	190*	35	4
Pd/Cu-Pt	41	22.8	30*	38*	48*	25	5
Pt in ｛Ni_{24}｝ coordination cage	----	48	60	-----	------	58	6
C-$Au_{98.2}Pt_{1.8}$ NPs	100_{Au}	22	35*	-----	-----	----	7
Pt-Pd@NPA	37.5	28.1	-----	-----	68*	31.2	8
Ni-NCNFs-Pt	280	47	62*	88*	130*	31	9
PtCo/CNFs	212.3	63	80*	-----	-----	28	10
Pt200-VGNSAs	41.92_{Pt}	60	80*	100*	150*	28.5	11
PtCoFe@CN	285	45	-----	-----	-----	36	12

References

1. T. F. Jaramillo, K. P. Jørgensen, J. Bonde, J. H. Nielsen, S. Horch and I. Chorkendorff, *Science*, 2007, **317**, 100–102.
2. N. Cheng, S. Stambula, D. Wang, M. N. Banis, J. Liu, A. Riese, B. Xiao, R. Li, T. K. Sham, L. M. Liu, G. A. Botton and X. Sun, *Nat. Commun.*, 2016, **7**, 13638.
3. H. Zhang, P. An, W. Zhou, B. Y. Guan, P. Zhang, J. Dong and X. W. Lou, *Sci. Adv.*, 2018, **4**, 6657.
4. J. Li, F. Li, S. X. Guo, J. Zhang and J. Ma, *ACS Appl. Mater. Inter.*, 2017, **9**, 8151-8160.
5. T. Chao, X. Luo, W. Chen, B. Jiang, J. Ge, Y. Lin, G. Wu, X. Wang, Y. Hu, Z. Zhuang, Y. Wu, X. Hong and Y. Li, *Angew. Chem.*, 2017, **56**, 16047-16051.
6. S. Wang, X. Gao, X. Hang, X. Zhu, H. Han, W. Liao and W. Chen, *J. Am. Chem. Soc.*, 2016, **138**, 16236-16239.
7. Z. Xi, H. Lv, D. P. Erdosy, D. Su, Q. Li, C. Yu, J. Li and S. Sun, *Nanoscale*, 2017, **9**, 7745-7749.
8. C. Yang, L. Hao, W. Zhou, J. Zeng and C. Xu, *J. Mater. Chem. A*, 2018, **6**, 14281-14290.
9. M. Li, Y. Zhu, N. Song, C. Wang and X. Lu, *J. Colloid Interf. Sci.*, 2018, **514**, 199-207.
10. T. Yang, H. Zhu, M. Wan, L. Dong, M. Zhang and M. Du, *Chem. Commun.*, 2016, **52**, 990-993.
11. B. Jiang, Z. Tang, L. Fan, H. Lin, S. Lu, Y. Li and M. Shao, *J. Mater. Chem. A*, 2017, **5**, 21903-21908
12. J. Chen, Y. Yang, J. Su, P. Jiang, G. Xia and Q. Chen, *ACS Appl. Mater. Inter.*, 2017, **9**, 3596-3601.